JOURNAL OF SOLID STATE CHEMISTRY 96, 192–198 (1992)

# A Completely Suppressed Jahn–Teller Effect in the Structure of Hexaaquachromium(II) Hexafluorosilicate

F. ALBERT COTTON AND LARRY R. FALVELLO

*Department of Chemistry and Laboratory for Molecular Structure and Bonding, Texas A&M University, College Station, Texas 77843-3255*

AND CARLOS A. MURILLO AND JAIME F. QUESADA

*Escuela de Química, Universidad de Costa Rica, Ciudad Universitaria, Costa Rica*

Received July 29, 1991

DEDICATED TO PROFESSOR PAUL HAGENMULLER ON HIS 70th BIRTHDAY

The structure of $[Cr(H_2O)_6]SiF_6$, a chromium(II) compound with homoleptic coordination, is reported. Hexaaquachromium(II) hexafluorosilicate crystallizes in space group $R\bar{3}$ with $a = 9.406(3)$ Å, $c = 9.762(5)$ Å, $V = 748.0(7)$ Å$^3$, and $Z = 3$. The $[Cr(H_2O)_6]^{2+}$ cation has $\bar{3}$ symmetry and is essentially a regular octahedron, therefore showing no Jahn–Teller distortion. The relationship of the $[Cr(H_2O)_6]^{2+}$ ion in this compound to other $[M(H_2O)_6]^{2+}$ ions ($M$ = Cr, V, Mn) is briefly discussed. 

## Introduction

It is generally observed that when a metal ion is in a cubic environment and its $e_{2g}$ orbitals have an odd number of electrons, there is a distortion of the geometry of the molecule to break the degeneracy of such orbitals. This is accounted for by the Jahn–Teller theorem (*1*). An abundance of examples are known for the high spin $d^4$ and $d^9$ systems in an "octahedral" environment, with compounds of $Cr^{2+}$ and $Cu^{2+}$ being the most common (*2*).

In our laboratories, we have been interested in the effects of crystal packing forces, especially rigid networks of hydrogen bonds, on ions subject to the Jahn–Teller effect. We have investigated the changes in the geometry of $Cr^{2+}$ when $Zn^{2+}$ is added over various composition ranges to the (Cr, Zn) saccharinate hexahydrate (*3*) and the (Cr, Zn) nicotinate tetrahydrate systems (*4*). However, in those cases, there is only a pseudo-octahedral arrangement of atoms around the chromium atom with four Cr–O bonds and two Cr–N bonds. Nevertheless, in the pure chromium compounds, there is a major difference in the lengths of the two sets of Cr–O bonds (close to 0.35 Å). For the (Cr, Zn) saccharinate, over the whole range of composition this difference is progressively reduced and the chromium atom is finally forced to occupy a nearly "undistorted" position within the crystal. For the nicotinate systems, introduction of Cr into the pure Zn compound up to 75% causes

0022-4596/92 $3.00

only a slight discrepancy in the two *M*–O distances. However, the pure chromium nicotinate shows a large difference, namely, 0.428 Å.

These results have prompted us to look at some homoleptic complexes of chromium(II). Even though the aqueous chemistry of this metal ion has been studied for years, the number of crystal structures containing the hexaaquachromium(II) ion is rather small. One of the few examples is the structure of the Tutton Salt (*5*), in which the expected distorted octahedron was observed.

In an effort to provide more insight into these systems, we decided to look at the structures of other compounds containing the hexaaquachromium(II) ion. One of them is the focus of attention in this paper, namely the one with the hexafluorosilicate anion. Several other crystal structures containing this anion and *M*(II) species had been investigated, namely those for *M* = Mg (*6*), Mn (*7*), Fe (*8*), Co (*9*), Ni (*9*), Cu (*10*), and Zn (*9*).

The structures of many of them are closely related, showing columns built up of alternating $[M(H_2O)_6]^{2+}$ and $SiF_6^{2-}$ octahedra, with both being essentially regular. However, static and dynamic crystal-field effects have been reported (*11*), as well as the formation of other phases (*12*).

The structure of the copper compound (*10*) deviates from the rest in that it shows both regular octahedra for the $[Cu(H_2O)_6]^{2+}$ ion as well as tetragonally distorted octahedra. This appears to be the first well-documented example of an undistorted $Cu^{2+}$ ion in an octahedral environment, the allegedly undistorted case of $K_2PbCu(NO_2)_6$ (*13*) being open to question.

## Experimental

In all cases in which chromium(II) solutions were used, standard Schlenk procedures where employed with nitrogen used as the inert gas. Solvents were deoxygenated and kept under nitrogen.

### *Preparation of Hexafluorosilicic Acid*

In a polyethylene flask, 60 mL of 40–45% HF (Merck) was diluted to a volume of 240 mL. To this solution was added an excess (50 g) of silica gel, TLC grade (Merck). This was stirred at room temperature for two days, filtered and concentrated under vacuum to two-thirds of the original volume.

### *Preparation of Hexaaquachromium*(II) *Hexafluorosilicate*

To 1.70 g chromium metal powder was added 5 mL of hexafluorosilicic acid and 20 mL of water. The mixture was stirred for 4 h at ca. 60°. Then it was filtered with silica gel on the fritted funnel. The solution was concentrated to 50% of its original volume, and a layer of 10 mL of ethanol was carefully added. After one week at 0°, blue crystals were collected.

### *Diffraction Analysis*

A block-shaped crystal of $[Cr(H_2O)_6]SiF_6$ was removed from the Schlenk tube under a continuous stream of argon and was rapidly encased in epoxy cement at the end of a glass fiber. Although exposure to air was thus limited to a few seconds, we observed the rapid adsorption of water on the surface of the crystal. In the first hours after mounting the crystal, we observed on diffraction photos the presence of a small amount of powder in addition to the strong diffraction pattern from the principal crystal. After a period of approximately half a day, the secondary diffraction pattern had disappeared, leaving the strong single-crystal pattern as the only observable diffraction of X rays from the sample. We observed by visual inspection at this point that the layer of epoxy about the crystal had contracted during its final setting. We concluded that a surface layer of powder or amorphous material had

been formed following deliquescence during the mounting and that the surface material had been absorbed or otherwise dispersed by the epoxy as it set. In any event, we began the diffraction studies for the purpose of structure analysis *after* the diffraction pattern from the sample was clearly seen from photographs to be a single-crystal pattern of excellent quality.

The crystal structure of $[Cr(H_2O)_6]SiF_6$ is essentially identical to the common structure found for many other hexafluorosilicates reported previously. Nevertheless, we conducted this structure analysis from the beginning, without prejudice from the structure reports already in the literature.

We used well-established procedures for the determination of the geometrical parameters of the crystal structure (*14*). The lattice was found to be metrically rhombohedral. We took normal-beam partial rotation photos of 6 axes: *a*, *b*, *c*, [210], [120], [$\bar{1}$11] (using the triply primitive hexagonal setting). All of the photos displayed clearly an absence of mirror symmetry, consistent with the Laue group $\bar{3}$. In addition, we used the photographs to verify the lattice repeats along the axes photographed. Crystal data are summarized in Table I.

For intensity data collection, we first gathered a hemisphere of data in the bisecting position ($\psi = 0$). In addition, the same hemisphere of data was gathered again at $\psi = 5°$. We saw no indication of important changes either in the data set as a whole or in any individual reflection from one azimuth setting to the other. Full azimuthal scans of five reflections were made for use in an absorption correction.

For data reduction, the application of absorption corrections (*15*) was followed by the averaging of equivalent data and the derivation of structure factors. Since there were six independent measurements of each unique reflection, we discarded any observation that was inconsistent with the remaining five. A total of 36 measurements (out of 2785) were thus omitted during this stage. The residual for the averaging of data was 0.024 (*16*).

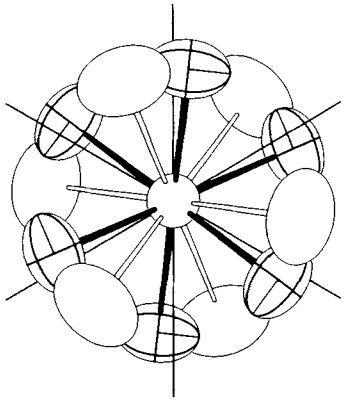

FIG. 1. Non-perspective ORTEP drawing of the disordered congeneric $SiF_6^{2-}$ ions in the crystal structure of $[Cr(H_2O)_6]SiF_6$. The view direction is along the *c*-axis. All atoms are represented by their 50% probability ellipsoids. Atom F(1) and its symmetry relatives are drawn with boundary and principal ellipses as well as front principal axes. For atom F(2) only the boundary ellipse is drawn. Lines represent the form of axes {210}.

The structure was solved by inspection of a Patterson map and was developed routinely. The $SiF_6^{2-}$ anion was found to be disordered with a single Si position surrounded by two sets of fluorine atoms. We refined a population parameter during isotropic refinement; its value at convergence gave a population of 0.533(15) for F(1). In the final, anisotropic refinement, we fixed the populations of F(1) and F(2) at 0.55 and 0.45, respectively. The structure of the anion is shown in Fig. 1.

The hexaaquachromium(II) ion was found to be fully ordered; its structure is depicted in Fig. 2. The hydrogen atoms were located in a difference Fourier map. They were refined initially with loose geometrical restraints on the O–H distances. In the final refinement, the geometrical restraints were removed. A single isotropic displacement parameter was refined for the two crystallographically independent hydrogen atoms.

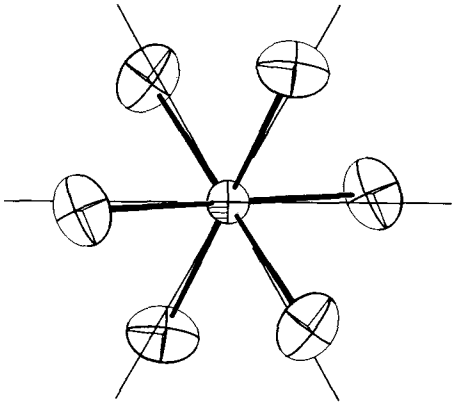

FIG. 2. Non-perspective ORTEP drawing of the cationic complex $[Cr(H_2O)_6]^{2+}$ from the crystal structure of $[(Cr(H_2O)_6]SiF_6$. All atoms are represented by their 50% probability ellipsoids. The view direction is from the positive *c*-axis to the origin. Lines are drawn along the form of zone axes ⟨100⟩.

In the final refinement, a total of 39 parameters were fitted to 472 unique data for a data-to-parameter ratio of 12 : 1. The final residuals are given in Table I. There were no significant variations of residuals as functions of $|F_{obs}|$, sin $\theta/\lambda$, or indices. We found that unit weights gave the best distribution of error as a function of $|F_o|$, and so unit weights were used for the final refinement.

## Results and Discussion

Positional parameters along with equivalent isotropic displacement parameters are listed in Table II. The general features of this structure have been discussed above and in an earlier report (*9*). Figure 3 depicts a portion of the extended structure showing the hydrogen-bond pattern.

The most remarkable feature of this structure is the appearance, for the first time, of an almost perfect octahedron around a high-spin six-coordinate chromium(II) ion. The symmetry of the space group requires that all Cr-to-O distances be identical. While it does not call for equality of all of the bond angles, it can be seen in Table III that they are all very close to the ideal value of 90°. This is in clear contrast with the usual occurrence of highly distorted high-spin $Cr^{2+}$ compounds in accordance with the Jahn–Teller effect (*2, 5*).

We have shown before that this distortion, normally manifested as a descent to tetragonal symmetry with an elongation of one pair of *trans* metal to ligand bonds, can be tempered in the solid state by changing the environment around the Jahn–Teller active species. We have done it in the past by addition of non-active species. Such is the case in the formation of solid solutions in the aqueous (Cr, Zn) saccharinate (*3*) and the (Cr, Zn) nicotinate (*4*) systems. It was found there that the hydrogen bonds play a

TABLE I

CRYSTAL DATA FOR $[Cr(H_2O)_6]SiF_6$

| | |
|---|---|
| Formula | $CrSiF_6O_6H_{12}$ |
| Formula weight | 302.2 |
| Space group | $R\bar{3}$ |
| Systematic absences | $(hkl)$: $-h + k + l \neq 3n$ |
| $a$, Å | 9.406(3) |
| $c$, Å | 9.762(5) |
| $V$, Å$^3$ | 748.0(7) |
| $Z$ | 3 |
| $d_{calc}$, g/cm$^3$ | 2.012 |
| Crystal size, mm | 0.77 × 0.77 × 0.74 |
| $\mu(MoK_\alpha)$, cm$^{-1}$ | 14.21 |
| Obsd. transmission factors, max., min. | 1.00, 0.98 |
| Data collection instrument | P3/F Equivalent |
| Radiation (monochromated in incident beam) | $MoK_\alpha(\lambda_\alpha^- = 0.71073$ Å) |
| Orientation reflections: number, range ($2\theta$), deg. | 25, 23.3–34.5 |
| Temperature, °C. | 20 ± 1 |
| Scan method | $\omega$–$2\theta$ |
| Data col. range, $2\theta$, deg. | 4.0–60.0 |
| Reflections collected | $(+h, \pm k, \pm l)$ |
| No. unique data | 481 |
| No. data with $F_o^2 > 3\,\sigma\,(F_o^2)$ | 472 |
| Number of parameters refined, final cycle | 39 |
| Weighting scheme | unit weights |
| $R^a$ | 0.0389 |
| Quality-of-fit indicator$^b$ | 1.176 |
| Largest shift/esd, final cycle | 0.03 |
| Largest difference peaks, e/Å$^3$ | 0.443, −0.427 |

[a] $R = \Sigma||F_o| - |F_c||/\Sigma|F_o|$.

[b] Quality-of-fit = $[\Sigma w(|F_o| - |F_c|)^2/(N_{obs} - N_{parameters})]^{1/2}$.

TABLE II

POSITIONAL PARAMETERS AND EQUIVALENT ISOTROPIC DISPLACEMENT PARAMETERS AND THEIR ESTIMATED STANDARD DEVIATIONS FOR $[Cr(H_2O)_6]SiF_6$

| Atom | $x$ | $y$ | $z$ | $B$(Å$^2$) |
|---|---|---|---|---|
| Cr(1) | 0.000 | 0.000 | 0.000 | 1.789(9) |
| Si(1) | 0.000 | 0.000 | 0.500 | 2.36(2) |
| O(1) | 0.1748(3) | 0.1880(2) | 0.1260(2) | 4.21(5) |
| F(1)[a] | 0.1662(4) | 0.0693(4) | 0.4001(3) | 4.43(8) |
| F(2)[a] | 0.1534(5) | 0.1366(5) | 0.3996(4) | 4.8(1) |
| H(1) | 0.206(6) | 0.158(6) | 0.228(4) | 8(1)[b] |
| H(2) | 0.138(6) | 0.274(6) | 0.118(5) | 8(1)[b] |

[a] Multiplicities for F(1) and F(2) are 0.55 and 0.45, respectively.

[b] A single isotropic displacement parameter was used for the two hydrogen atoms. Anisotropically refined atoms are given in the form of the equivalent isotropic displacement parameter defined as: $(4/3)[a^2\beta_{11} + b^2\beta_{22} + c^2\beta_{33} + ab(\cos \text{gamma})\beta_{12} + ac(\cos \text{beta})\beta_{13} + bc(\cos \text{alpha})\beta_{23}]$.

very important role in the observed modification of the $M$–O distances. We have no doubt that they must also be very important in forcing the observed structure of the title compound.

One can possibly argue that the appearance of a unique Cr–O bond length is the result of the average of two or more unresolved distances. It is conceivable that there is a dynamic distortion of the complex in the crystal. However, the diffraction data analysis strongly supports the conclusion that there is a unique Cr–O bond length. The displacement parameters are inconsistent with the idea of movement in the direction of the bond, and in fact suggest that the largest motion of the oxygen atom is perpendicular to the bond, as seen in Fig. 2. A possible elongation of the Cr–O bond would also be very detrimental to the extended array of hydrogen bonds.

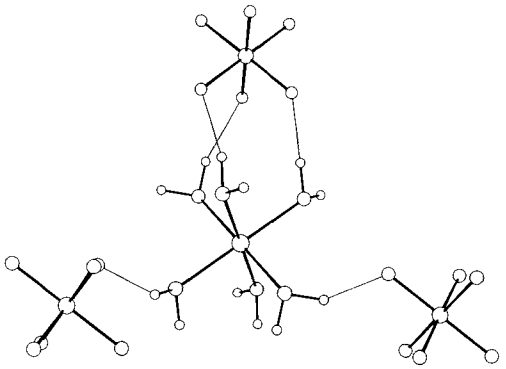

FIG. 3. ORTEP perspective drawing of a portion of the extended structure of $[Cr(H_2O)_6]SiF_6$, showing the hydrogen-bonding pattern. The crystallographic $c$-axis is vertical in the plane of the paper. The chromium complex in this drawing is centered at (000). The $SiF_6^{2-}$ ion above it (Si at (001/2)) is drawn with F(1) bonded to Si. The $SiF_6^{2-}$ anions to the left (Si at (2/3,1/3, – 1/6)) and to the right (Si at ( – 1/3,1/3, – 1/6)) are drawn with F(2) bound to the Si atom.

The presence of a fully ordered cation is also supported by the appearance of the hydrogen atoms on a difference Fourier map and their successful refinement. Conclusive evidence for the single occupation of the oxygen atom site comes from the difference Fourier map, a section of which is shown in Fig. 4. The difference Fourier map shown in the figure was made with $F_{calc}$ taken from a model in which the oxygen and hydrogen atoms had been removed. (All other sites had their final refined parameter values). As the figure shows, the oxygen site has no more extent in the direction of the Cr–O bond—the direction of possible Jahn–Teller

TABLE III

DERIVED DISTANCES (Å) AND ANGLES (DEG.) AND THEIR ESTIMATED STANDARD DEVIATIONS FOR $[Cr(H_2O)_6]SiF_6$

| Covalent distances and bond angles | | | |
|---|---|---|---|
| Cr(1)–O(1) | 2.106(2) | *cis*-O(1)–Cr(1)–O(1) | 90.66(9)<br>89.34(9) |
| Si(1)–F(1) | 1.673(3) | *cis*-F(1)–Si(1)–F(1) | 90.5(2)<br>89.5(2) |
| Si(1)–F(2) | 1.685(3) | *cis*-F(2)–Si(1)–F(2) | 90.4(2)<br>89.6(2) |
| O(1)–H(1) | 1.11(5) | Cr(1)–O(1)–H(1) | 120(2) |
| O(1)–H(2) | 1.02(7) | Cr(1)–O(1)–H(2) | 101(2) |
| | | H(1)–O(1)–H(2) | 120(4) |
| | | Hydrogen bonds | |
| *A*–*B* · · · *C* | *A* · · · *C* | Angle at *B* | *C* coords. |
| O(1)–H(1) · · · F(1) | 2.885(4) | 157(4) | *x*,*y*,*z* |
| O(1)–H(2) · · · F(1) | 2.758(3) | 137(4) | $y - x + 1/3, -x + 2/3, z - 1/3$ |
| O(1)–H(1) · · · F(2) | 2.704(4) | 143(5) | *x*,*y*,*z* |
| O(1)–H(2) · · · F(2) | 2.720(4) | 118(4) | $y - x + 1/3, -x + 2/3, z - 1/3$ |

distortion—than it has in any other direction.

The presence of a configuration which does not allow the chromium(II) atom to reach its normal energy minimum is probably the cause of the highly efflorescent behavior, briefly discussed in the Experimental Section, of the hexaaquachromium(II) hexafluorosilicate compound. When exposed to water, even in the form of ambient humidity, the system rapidly takes on water; undoubtedly the molecules in the liquid phase have the configurational energy minima prescribed by the Jahn–Teller theorem.

It is remarkable, considering their great importance, that there is only very limited structural information on the hexaquo ions of the divalent transition metals, $[M(H_2O)_6]^{2+}$; meaningful comparisons of the present results with those of other related compounds is thus nearly impossible. It is not possible to compare the Cr–O bond length in $[Cr(H_2O)_6]SiF_6$ with those in the analogous V and Mn compounds to see whether it is, as expected, approximately

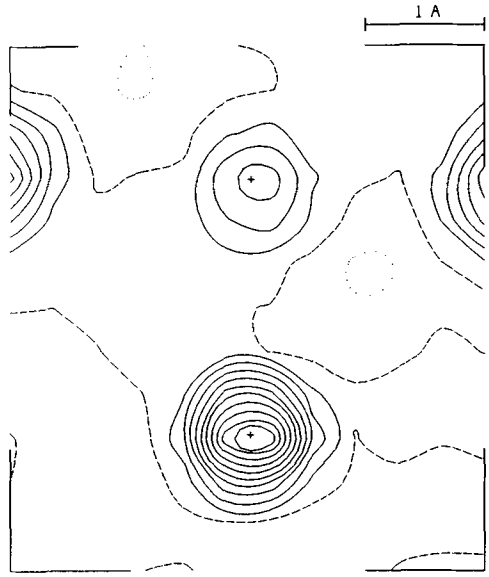


FIG. 4. Contoured difference Fourier section from the X-ray diffraction analysis of $[Cr(H_2O)_6]SiF_6$. The conditions under which the map was calculated are described in the text. The plus sign (+) in the upper section of the plot represents the Cr atom position, and the (+) in the lower portion of the plot represents the final refined coordinates of the oxygen atom. Contours are drawn at increments of 0.65 e/Å$^3$.

halfway in between because the structures of the V and Mn compounds are unavailable. It seems clearly risky to attempt to compare dimensions from one type of structure to another. For the Cr Tutton salt, the average Cr–O distance is 2.167 Å as compared to 2.106 Å in $[Cr(H_2O)_6]SiF_6$. This discrepancy could mean that the averaged value for a Jahn–Teller distorted $[Cr(H_2O)_6]^{2+}$ ion is truly greater than that for the undistorted case, but more likely it means that the strong forces in $[Cr(H_2O)_6]SiF_6$ that suppress the Jahn–Teller effect also cause a net compression of the $[Cr(H_2O)_6]^{2+}$ ion as a whole.

One more interesting aspect of this compound that remains to be examined is how its electronic properties (magnetic and spectroscopic) will differ from those of compounds in which the $[Cr(H_2O)_6]^{2+}$ ion exhibits its usual tetragonal distortion. With the aid of crystal-field theory, the relationship between the two cases can be at least approximately predicted. The degree to which these will be experimentally confirmed should be of interest.

## Acknowledgments

We are grateful to The Robert A. Welch Foundation under Grant A-494 for support of work at Texas A&M University, and to Vicerrectoría de Investigación, U.C.R. (Grant 115-87-006) for support at the University of Costa Rica. We also thank Dr. Richard Staples for assistance with the reduction of X-ray data.

## References

1. (*a*) H. JAHN AND E. TELLER, *Phys. Rev.* **49,** 874 (1936); (*b*) H. JAHN AND E. TELLER, *Proc. R. Soc. London, A:* **161,** 220 (1937).
2. (*a*) F. A. COTTON AND G. WILKINSON, "Advanced Inorganic Chemistry," 5th ed., Wiley, New York (1988); (*b*) J. B. BERSUKER, "The Jahn–Teller Effect and Vibronic Interactions in Modern Chemistry," Plenum Press, New York (1984).
3. F. A. COTTON, L. R. FALVELLO, C. A. MURILLO, AND G. VALLE, *Z. Anorg. Allg. Chem.* **540/541,** 67 (1986).
4. F. A. COTTON, L. R. FALVELLO, E. L. OHLHAUSEN, C. A. MURILLO, AND J. F. QUESADA, *Z. Anorg. Allg. Chem.*, in press.
5. B. N. FIGGIS, E. S. KUCHARSKI, AND P. A. REYNOLDS, *Acta Crystallogr., Sect. B: Struct. Sci.* **B46,** 577 (1990).
6. S. SYOYAMA AND K. OSAKI, *Acta Crystallogr., Sect. B: Struct. Crystallogr. Cryst. Chem.* **B28,** 2626 (1972).
7. E. KODERA, A. TORII, K. OSAKI, AND T. WATANABE´, *J. Phys. Soc. Jpn.* **32,** 863 (1972).
8. W. C. HAMILTON, *Acta Crystallogr.* **15,** 353 (1962).
9. S. RAY, A. ZALKIN AND D. H. TEMPLETON, *Acta Crystallogr., Sect. B: Struct. Crystallogr. Cryst. Chem.* **B29,** 2741 (1973).
10. S. RAY, A. ZALKIN AND D. H. TEMPLETON, *Acta Crystallogr., Sect. B: Struct. Crystallogr. Cryst. Chem.* **B29,** 2748 (1973).
11. D. C. PRICE, *Can. J. Phys.* **65,** 1280 (1987).
12. F. A. BOIKO, G. YU. BOCHKOVOVAYA, A. M. BYKOV, V. L. KOVARSKY, N. E. PISMENOVA, V. G. KSNOFONTOV, I. V. RUBAN, R. YA. SUKHAREVSKY, E. O. TSYBULSKY, AND G. E. SHATALOVA, *Ferroelectrics* **75,** 431 (1987).
13. (*a*) H. ELLIOT, B. J. HATHAWAY, AND R. C. SLADE, *Inorg. Chem.* **5,** 669 (1966); (*b*) D. REINEN, C. FRIEBEL, AND K. P. REETZ, *J. Solid State Chem.* **4,** 103 (1972).
14. F. A. COTTON, B. A. FRENZ, G. DEGANELLO, AND A. SHAVER, *J. Organomet. Chem.* **50,** 277 (1973).
15. A. C. T. NORTH, D. C. PHILLIPS, AND F. S. MATHEWS *Acta Crystallogr., Sect. A: Cryst. Phys. Diffr. Theor. Gen. Crystallogr.* **A24,** 351 (1968).
16. Computing was done on a Data General Eclipse computer with the SHELXTL package, and on a Local Area VAX cluster (VMS V5.2) with the program SHELX-76 and with the commercial package SDP/V V3.0.